Synthesis and study of electrical properties of Li$_2$O modified P$_2$O$_5$-ZnO-Na$_2$O glasses

N. F. Osman [a], M. M. Elokr [b], L. I. Soliman [c], H. A. Zayed [d]

[a] Physics Department, Modern Academy for Engineering and Technology in Maadi, Cairo, Egypt
[b] Physics Department, Faculty of Science, Al-Azhar University, Cairo, Egypt
[c] National Research Center, Dokki, Cairo, Egypt
[d] Physics Department, Faculty of Women, Ain Shams University, Cairo, Egypt

Abstract

The transparent glasses of composition 40P$_2$O$_5$-20ZnO-(40-x)Na$_2$O-xLi$_2$O have been prepared using conventional melt quenching technique (where $0 \leq x \leq 25$ Li$_2$O mol. %). The amorphous nature of the prepared glass samples is confirmed by x-ray powder diffraction (XRD). By increasing the Li$_2$O content, the density and oxygen packing density increase while the molar volume decreases which indicates that the structure is more compact. The differential thermal analysis (DTA) studies showes that 15 mol.% Li$_2$O glass sample has the highest thermal stability and the glass transition temperature (T$_g$) decreases as the content of Li$_2$O increases till 25 mol.% Li$_2$O . The ac and dc electrical conductivities and dielectric constants of the prepared glass samples have been investigated. It is found that the dc conductivity increases with the concentration of Li$_2$O mol.% and the temperature dependence of the dc conductivity at low temperature (303 – 383 K) and at high temperature (403 – 473 K) obey the Arrhenius law. The activation energies ΔE_{dc1} (at high temperatures) and ΔE_{dc2} (at low temperatures) were determined. The values of σ_{dc} can be obtained also from the impedance study at different temperatures and different concentrations using Cole-Cole plot. To determine the conduction mechanism, the ac conductivity and its frequency exponent (s) have been analyzed by correlated barrier hoping model (CBH). It is found that s has values between 0.89-0.996; consequently. The correlated barrier hopping (CBH) seems to be the most interesting model related to the obtained results. Real and imaginary parts of dielectric constant (ε' and ε'') have been found to decrease with increasing frequency and temperature and this result would be discussed by means of dielectric polarization mechanism of material. The maximum value of the maximum barrier height W_m obtained from Guitini equation was found to increase with increasing of Li$_2$O mol. %.

Key words: phosphate glasses, structure properties, electrical properties.

*__Corresponding Author__ : dr.naglaa_fathy85@yahoo.com

Introduction

Recently, the synthesis and the study properties of phosphate glasses have attracted much attention because of their potential technological applications. Phosphate glasses possess a series of interesting and unique physical properties better than other glasses such as transparency at room temperature, sufficient strength, hardness, excellent corrosion resistance, low melting and softening

temperature, high thermal expansion, high electrical conductivity, low glass transition temperature, ultraviolet and far-infrared transition and other optical characteristics **[Yahia H. Elbashar et al. (2016), R. K. Brow (2000), Samir Y. Marzouk et al (2009), A. Bhide et al (2007), I. Abrahams et al (2000)]**. For laser application phosphate glasses used as transmitting optical components, as modulators, for photonic switching and magneto-optic materials **[D. D. Ramteke et al (2017)]** and have been considered as a promising group of glasses for optical amplifiers, fibers, etc. **[A.V. Chandrasekhar et al (2003), Nehal Aboulfotoh et al (2014)].** Several studies have been shown that a chemical durability of phosphate based glasses can be improved by the addition of various oxides **[S. T. Reis et al (2001), D. E. Day et al (1998)]**. ZnO acts as a glass modifier, where Zn^{2+} occupies interstitial sites in glass network **[D. Carta et al (2009)]**. With the addition of ZnO to phosphate glasses, the P—O—P bonds are replaces by more chemically durable P—O—Zn bond **[R. K. Brow et al (1995)]** and also, it is interesting because the $ZnO – P_2O_5$ systems show unusual change in correlation between the structural and optical properties (e.g.: refractive index and ultraviolet absorption edge) at the metaphosphate composition **[P. M. V. Teja et al (2012)].** Among oxide glasses, sodium and lithium phosphate glasses are well known due to their variety of technological applications such as solid electrolytes for battery applications **[Paramjyot Komar Jha et al (2015), A. Yamano et al (2014)]**. Sodium phosphate glasses are in a great demand because of their strong glass forming nature, low crystallization and melting temperature. It is expected that the replacement of Na_2O by Li_2O in P_2O_5-ZnO based glasses exhibit better ionic conductivity due to smaller size of Li^+ ($0.76A^o$) as compared to Na^+ ($1.02A^o$). Recently the structural properties of $P_2O_5 – Na_2O – Li_2O$ glasses strongly depend on Na_2O and Li_2O content.

In literature we find that the dc and ac electrical conductivity of $P_2O_5 – ZnO – Na_2O – Li_2O$ glass system have not been studied extensively for this reason, the present work gives the preparation of $40P_2O_5$-$20ZnO$-$(40-x)Na_2O$-xLi_2O glasses containing varying concentration of Li_2O reaching to 25 mol.% and deals with the dc and ac electrical conductivity over a wide range of temperature and frequency to determine the possible conduction mechanisms and to determine the activation energy.

2. Experimental

2.1. Preparation of the glasses

The investigated glasses $40P_2O_5$-$20ZnO$-$(40-x)Na_2O$-xLi_2O ($0 \leq x \leq 25$) were prepared by the conventional melt quenching technique using high purity analytical grade chemicals $(NH_4)_2HPO_4$, ZnO, Na_2CO_3 and $LiCl$ as the raw material. The appropriate quantity of these chemicals was weighted and mixed in agate mortar and were hand ground for about one hour. The weighted batches were heated in an electric furnace at 673K for 1/2 h in porcelain crucibles to release the ammonia then melted at 1273K for 1 h with intermediate stirring to achieve the homogeneity of the melt. So, samples of the desired shape were obtained by quenching the melt at 623K on a stainless steel mold for 2h to eliminate the mechanical and thermal stresses produced during casting and left to cool to room temperature. The $40P_2O_5$-$20ZnO$-$(40-x)Na_2O$-xLi_2O glasses varied from 0 to 25 mol. % in steps of 5 mol. %.   The prepared glass samples were polished by silicon carbide water proof abrasive papers of various grades ranging between 320 and 1000 to achieve a good optical transparency samples.

2.2. X- ray Diffraction measurements (XRD)

The amorphous nature of synthesized glass samples was checked by PANalytical X'Pert PRO diffractometer using CuKα target of wavelength 1.5406 A^o and scanning rate 2 ^{0}/min. XRD patterns were recorded in 2θ range between 4 ^{0} and 80 ^{0}.

2.3. Density measurements

The density (ρ) of the glass samples were determined at room temperature by the standard Archimedes principle using toluene as an immersion liquid (ρ_x= 0.86455 gm. /cm^3). The density was obtained from the relation,

$$\rho = [W_a / (W_a - W_b)] \cdot \rho_x , \qquad\qquad (1)$$

Where, W_a is the weight of the glass sample in air, W_b is the weight of the glass sample when immersed in toluene. The relative error in these measurements was about 1 mg/cm^3. Also, the molar volume (V_M) and the oxygen packing density (OPD) of the glass samples were calculated by using the molecular weight (M) and density (ρ) according to the following relations.

$$V_M = M / \rho \qquad\qquad (2),$$

and
$$OPD = 1000 \cdot (\rho / M) \cdot n \qquad\qquad (3)$$

Where, n is the no. of oxygen atoms per formula unit.

2.4. Differential Thermal Analysis (DTA)

The glass transition temperature (T_g) and the crystallization temperature (T_C), were evaluated for all the glass samples by using SDT Q600 V20.9 and scanned at a heating rate 10 K/min.

2.5. Electrical measurements

The prepared samples of the $40P_2O_5$-$20ZnO$-$(40-x)Na_2O$-xLi_2O glasses were coated with silver paint on both sides for dc and ac electrical conductivity measurements and using a special designed holder.

The dc and ac electrical conductivity σ for the prepared samples was carried out in the temperature range (303 - 473 K). The sample temperature was measured and controlled by using a calibrated Chromel-Alumel thermocouple connected to (TCN4M-24R Aulonics-Korea) temperature controller. For ac electrical conductivity measurements a programmable automatic LCR bridge (Hioki, 3532-50) was used in a wide frequency range (50 Hz to 5 MHz).

3. Results and Discussion

3.1. X- ray Diffraction measurements (XRD)

The amorphous nature of the prepared glass samples is confirmed by x-ray powder diffraction (XRD) fig.1 **[H. A. Zayed et al (2019)].**
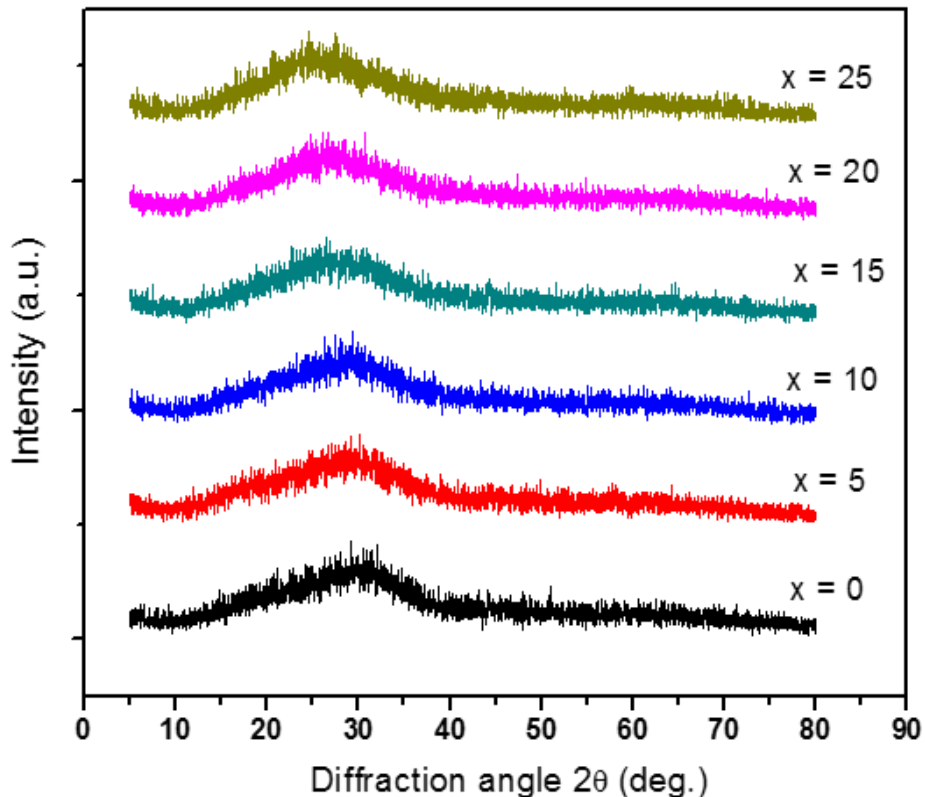
Fig.1: XRD patterns of the $40P_2O_5$-$20ZnO$-$(40-x)Na_2O$-xLi_2O glasses with different concentrations of Li_2O mol.%.

3.2. Density and molar volume

The values of density (ρ) and molar volume (V_M) of all the glass samples have been evaluated and their values are given in table 1. Density and oxygen packing density are found to increase with increasing the content of Li_2O in all glasses. This behavior of density is due to the electron negativity of Zn^+ (1.65) is the most bigger than Na^+ (0.93) and Li^+ (0.98) which is responsible to compact the glass network. Also, the field strength of Li_2O (0.21) attracts the oxygen ions more than Na_2O (0.17), leading to an increase in the density **[H. A. Zayed et al (2019)]**.

Table 1: Density (ρ), molar volume (V_M), and oxygen packing density (OPD) of the $40P_2O_5$-$20ZnO$-$(40-x)Na_2O$-xLi_2O glass samples.

Compositions of the $40P_2O_5$-$20ZnO$-$(40-x)$ Na_2O-xLi_2O glasses (X in mol. %)	Theoretical density $\rho_{th.}$ (gm./cm^3)	Experimental density $\rho_{exp.}$ (gm./cm^3)	Molar volume V_M (cm^3/mol.)	Oxygen packing density OPD (mol./litre)
0	2.680	2.690	36.37	71.48
5	2.710	2.7316	35.232	73.795
10	2.736	2.7711	33.906	76.132
15	2.778	2.8077	33.134	78.468
20	2.814	2.8492	32.089	81.025
25	2.860	2.8920	31.059	83.712

3.3. Differential Thermal Analysis (DTA)

The differential thermal analysis (DTA) was investigated previously and the characteristic temperatures are tabulated in table 2. It was found that as the concentration of Li_2O increases from 0 mol.% to 25 mol.%, the glass transition temperature T_g decreases because of Li_2O is a strong modifier which creates non-bridging oxygen (NBO). The non-bridging oxygen disrupt the long chains and break the chemical bonds. The value of glass thermal stability H' for the glass sample with Li_2O content 15 mol.% is found to be maximum, which indicates its highest thermal stability than other glasses **[H. A. Zayed et al (2019)]**.

Table 2: Thermal constants observed from DTA for the $40P_2O_5$-$20ZnO$-(40-x) Na_2O-xLi_2O glass samples.

Glass sample (X in mol. %)	Glass transition temp. T_g(K)	Crystallization temp. T_C(K)	Glass thermal stability H' = ΔT / T_g
0	558.08	623.01	0.116
5	551.15	617.1	0.120
10	548.02	616.1	0.124
15	545.6	615.6	0.128
20	545.5	614.6	0.126
25	546.7	615.2	0.125

3.4. Electrical conductivity

3.4.1. dc electrical conductivity

The temperature dependence of dc electrical conductivity of the $40P_2O_5$-$20ZnO$-(40-x)Na_2O-xLi_2O glasses ($0 \leq x \leq 25$ mol. % Li_2O) are shown in fig. 2. The data fit the Arrhenius equation $\sigma_{dc} = \sigma_o \exp(-E_a / kT)$, σ_o is the pre-exponential factor which including the charge carrier mobility and density of states, E_a is the thermal activation energy for conduction and k is the Boltzmann constant. There are two linear regions of conductivity that gave two activation energies ΔE_{dc1} for high temperatures (403-473K) region and ΔE_{dc2} for low temperatures (303-383K) region which arise from impurity scattering.
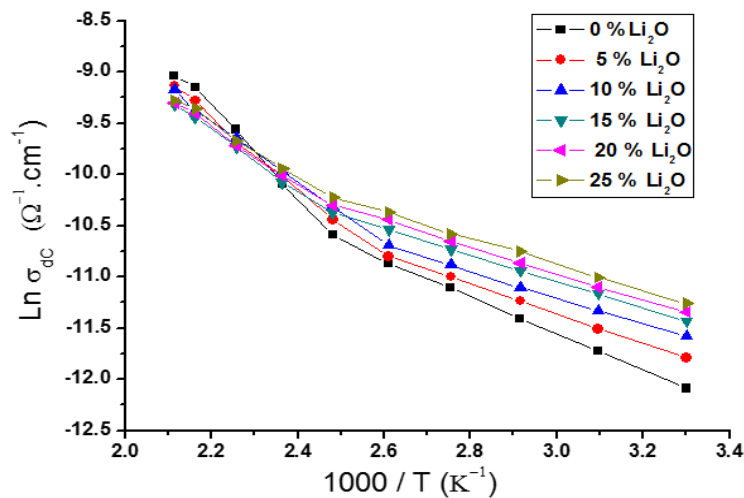

Fig. 2: The variation of Ln σ_{dc} versus 1000 / T for $40P_2O_5$-$20ZnO$-(40-x)Na_2O-xLi_2O glass samples at different composition of Li_2O mol.%.

The variation of σ_{dc} at room temperature and the activation energies ΔE_{dc1} and ΔE_{dc2} with the concentration of Li_2O (mol. %) are represented in fig.3. It is clear from fig.3 that σ_{dc} increases from 6.14×10^{-6} to 1.33×10^{-5} ($\Omega^{-1}.cm^{-1}$) with increasing of Li_2O content. In order to explain this behavior one must note that these quaternary glasses were fabricated by adding different amount of Li_2O to ternary zinc-sodium-phosphate glass. The sodium ions were gradually replaced by lithium ions because the amount of glass former P_2O_5 was fixed at 40 mol.% and glass modifier ZnO was fixed at 20 mol.%. Such behavior is likely to arise due to structural changes occurring in phosphate network. The activation energies calculated from analysis of Ln σ_{dc} versus $1000 / T$ plots is found to decrease with increasing Li_2O content to 15 mol. % and then a nearly constant trend with increasing Li_2O content.
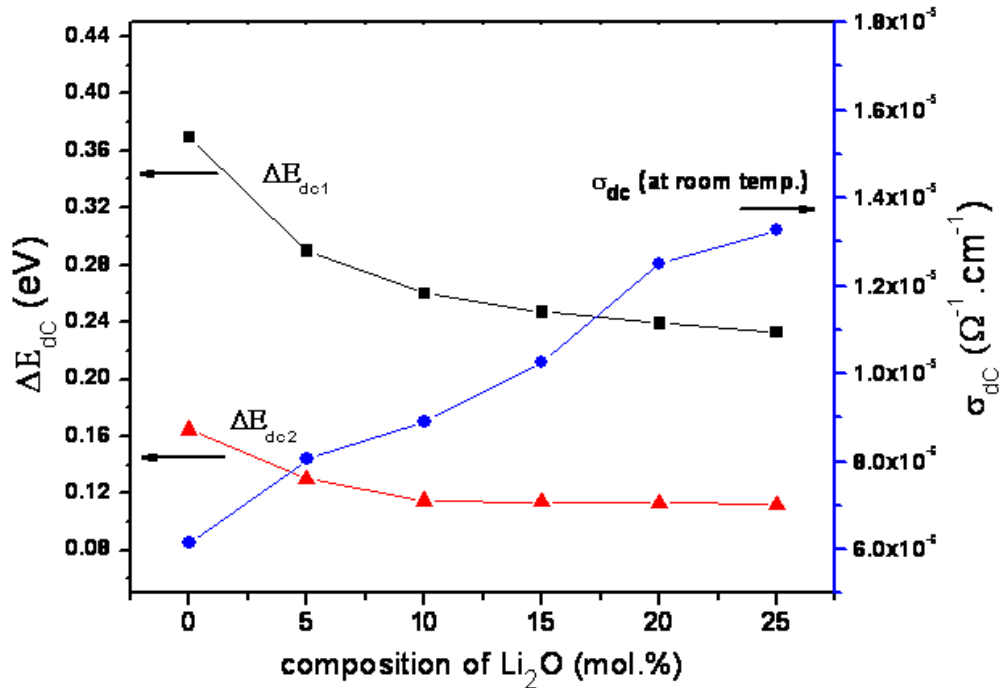

Fig. 3: The variation of activation energy ΔE_{dc1} and ΔE_{dc2} and σ_{dc} at room temperature with the composition of Li_2O mol. %.

3.4.2. ac electrical conductivity

The ac conductivity σ_{ac} can be described by eqn. 4. Where, σ_t is the total conductivity and σ_{dc} is the dc conductivity at zero frequency (w = 0). At very low frequency region σ_{dc} is independent of frequency and appears as a flat dc plateau in this region of frequency. The ac conductivity is approximately independent of the frequency at lower frequencies, but more frequency dependent in high frequency region. The ac conductivity follows the relation:

$$\sigma_{ac}(\omega) = \sigma_t - \sigma_{dc}(\omega = 0) \qquad (4)$$

In this relation, the dc conductivity is taken to represent the ac conductivity at ω tends to zero. The ac conductivity has been analyzed used Almond-West type power law with single exponent **[D. P. Almond et al. (1984)]**.

$$\sigma_{ac} = A \cdot \omega^s \tag{5}$$

Where A is a temperature dependent constant, $\omega = 2\pi f$ is the angular frequency and s is the frequency exponent which depend on temperature. Such a dependence on temperature determines the ac conduction mechanism and has been found to be material dependent.

3.4.2.1. Complex impedance analysis

Complex impedance is a powerful technique for the characterization of electrical properties of polycrystalline sample such as conductivity, dielectric behavior ….. etc. It may be used to explain the dynamics of mobile or bound charges in the grain or grain boundaries. The expression of real (Z') and imaginary (Z") components of the impedance (Z) can be expressed by the following relationships:

$$Z = Z' - jZ'' \tag{6}$$

$$Z' = Z \cos Q \tag{7}$$

$$Z'' = Z \sin Q \tag{8}$$

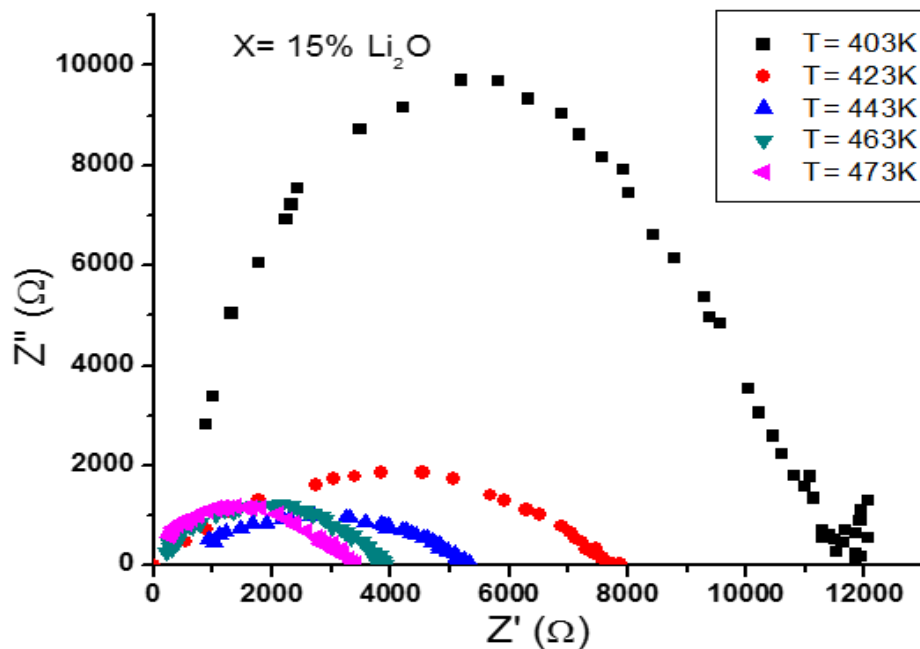Where $Q = 1 / [\, C \cdot Z \cdot (2\Pi f)\,]$

Fig 4: Cole-Cole plots of Z' and Z" for $40P_2O_5$-$20ZnO$-$(40-x)Na_2O$-xLi_2O glass samples Containing 15% Li_2O (mol. %) at different temperatures.

Fig.4 shows the plot of Z' versus Z" (Cole-Cole plot) for glass sample (with x = 15 mol% Li_2O) at different temperature, fig.5 Cole-Cole plots of Z' and Z" for glass samples with different compositions of Li_2O mol%. The impedance plots of all the samples were found to exhibit good single semicircle starting from the origin over the entire range of temperature and the composition studied. The absence of second semicircle in the complex impedance plots indicates that the glass samples have only grain effect to the conductivity mechanism at room temperature.
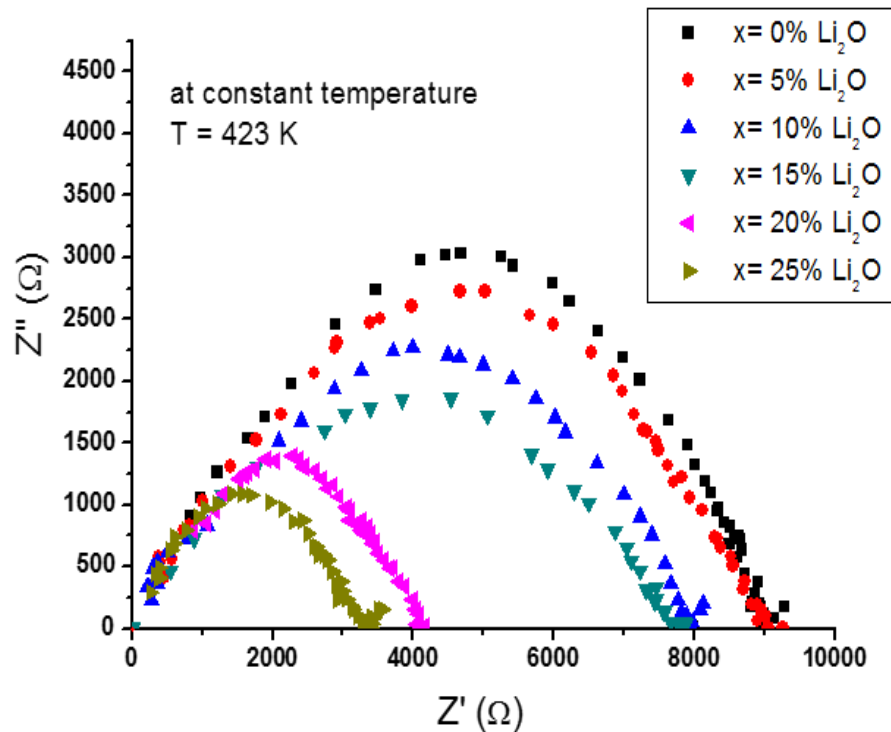

Fig. 5: Cole-Cole plots at 423 K for different concentrations of Li_2O mol%.

The values of dc conductivity were calculated by taking the intersection points of semicircles on the Z' axis **[M. J. Miah et al. (2016)]**. Figures.4, 5 illustrated that the diameter of the semicircle decreasing and the intersection points of the semicircles shifted to lower Z' values with increasing temperature and with increasing Li_2O content in glass samples which suggests that the value of grain resistance is decreasing and σ_{dc} increasing with increasing temperatures and the value of grain resistance is decreasing to minimum.

To compare the obtained data of σ_{dc} calculated from Cole-Cole and σ_{dc} calculated from σ_t versus frequency are listed in table 3. It is clear that σ_{dc} (Cole-Cole) and σ_{dc} (σ_t Vs f) approximately have same values.

Table 3: values of σ_{dc} (Cole-Cole) and σ_{dc} (σ_t Vs f) at different temperatures (for constant concentration

15% Li_2O mol. %).

T(k)	σ_{dc} (Cole-Cole)	σ_{dc} (σ_t Vs f)
403	$2.83 * 10^{-5}$	$3.136 * 10^{-5}$
423	$4.17 * 10^{-5}$	$4.190 * 10^{-5}$
443	$6.41 * 10^{-5}$	$6.706 * 10^{-5}$
463	$8.43 * 10^{-5}$	$8.524 * 10^{-5}$
373	$9.73 * 10^{-5}$	$9.708 * 10^{-5}$

3.4.2.2. Frequency and temperature dependence of ac electrical conductivity

Fig.6 shows the frequency dependence of ac electrical conductivity at different temperatures for the $40P_2O_5$-$20ZnO$-$(40-x)Na_2O$-xLi_2O glasses (with x = 15 mol. % Li_2O). The ac conductivity behavior of all the other glass samples (with x = 0, 5, 10, 20, 25 mol. % Li_2O) is qualitatively similar.

The increase of σ_{ac} with increasing frequency suggests that hoping conduction prevails and the increase of the applied frequency enhances the hopping of charge carriers between the localized states **[A. Ben Rasem et al. (2009)].**
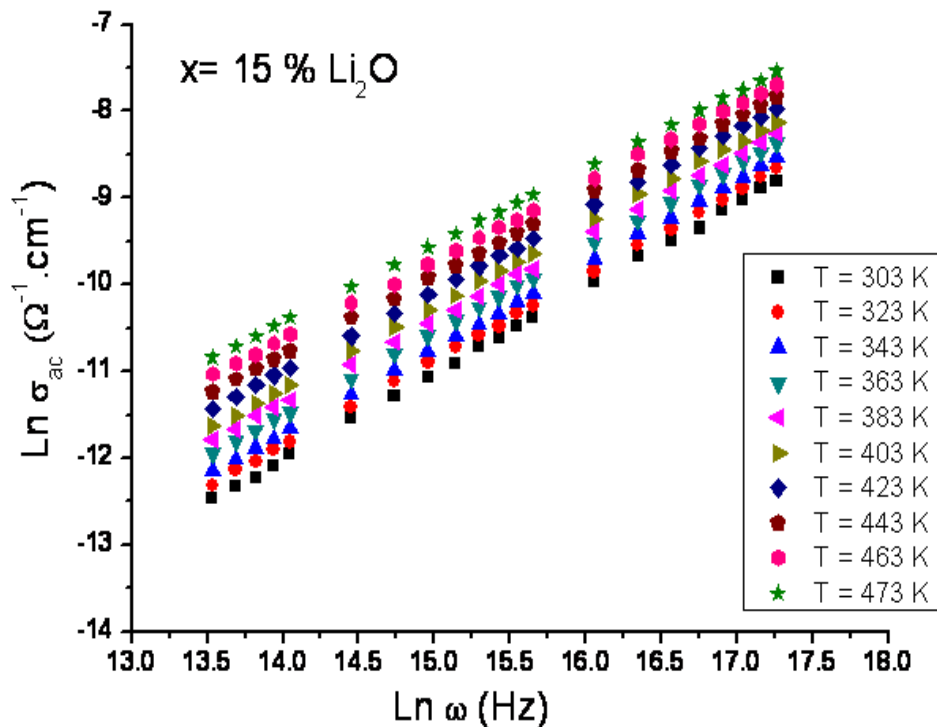
Fig.6: Frequency dependence of σ_{dc} for $40P_2O_5$-$20ZnO$-$(40-x)Na_2O$-xLi_2O glasses containing 15 mol% Li_2O at different temperatures.

The values of the exponent s (eqn.5) were calculated from the slopes of these lines at different temperatures. The temperature dependence of s for all the prepared glass samples with different concentrations is shown in fig.7 in which s decreases with increasing temperature and the concentration of the modifier oxide (Li_2O). Also it was found that for all the prepared glass samples s values are significantly lower than unity and lie between 0.89-0.996.

According to correlated barrier hopping (CBH) model values of s decrease with increasing temperatures, this is in good agreement with the obtained results, as shown in fig.7. Accordingly the frequency dependence of σ_{ac} can be explained in terms of CBH model. This model first developed by Pike **[G. E. Pike (1972)]** for single electron hoping and has been extended by Elliot and Chen **[S. R. Elliot (1978), R. H. Chen et al. (2006)]** for simultaneous two electron hoping.
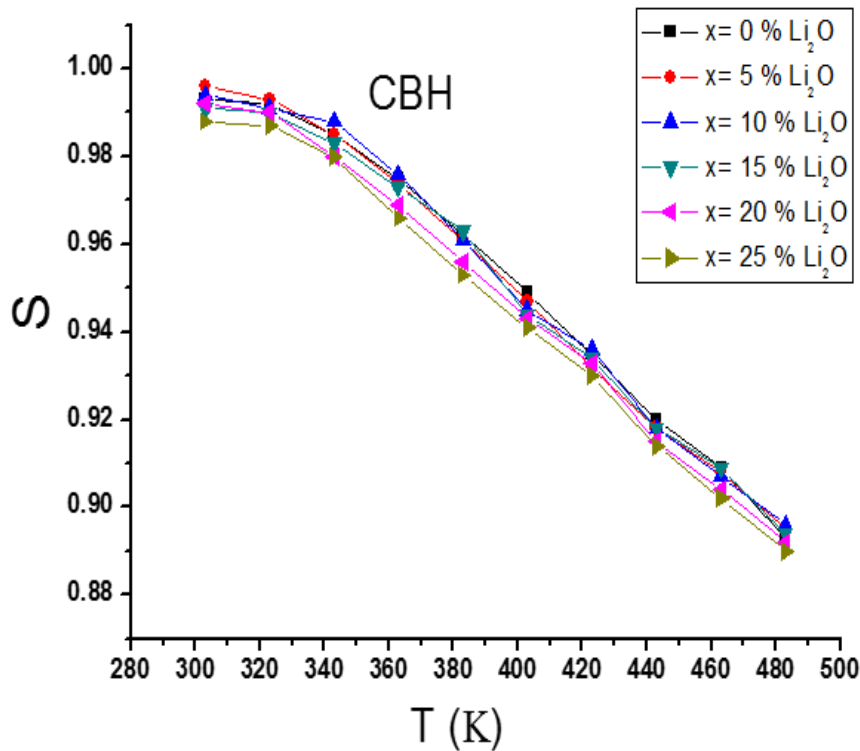

Fig.7: Temperature dependence of the frequency exponent S at different concentrations of Li_2O mol.%.

Fig.8 shows the variation of Ln σ_{ac} with the reciprocal of temperature 1000 / T in the investigated temperature range at different frequencies for the $40P_2O_5$-$20ZnO$-$(40-x)Na_2O$-xLi_2O glasses. This dependence of ac conductivity on temperature suggests that the ac conductivity is a thermally activated process. The value of the activation energies ΔE_{ac} has been calculated from the slope of Ln σ_{ac} versus 1000 / T curves. Fig. 9 shows the variation of the activation energies ΔE_{ac} with concentration of Li_2O mol% at different frequencies. It is found that the activation energies ΔE_{ac} decrease with increase of Li_2O concentration and the plot is found to exhibit minimum at X = 5 mol% Li_2O, also it is observed that the behavior of both ΔE_{dc} and ΔE_{ac} are almost the same, Such increase can be attributed to the contribution of the applied frequency to the conduction mechanism, which confirms the hopping conduction to be dominant mechanism **[Sh. A. Mansour et al. (2010)]**
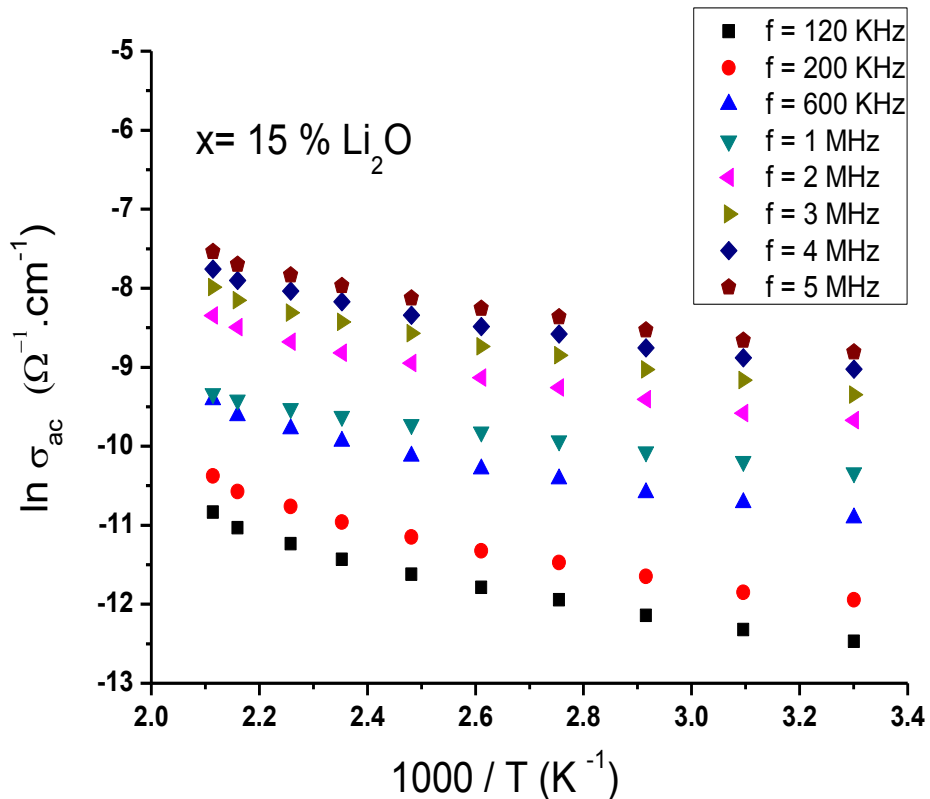

Fig.8: Temperature dependence of ac conductivity for glasses containing 15 mol% Li_2O at different frequencies.
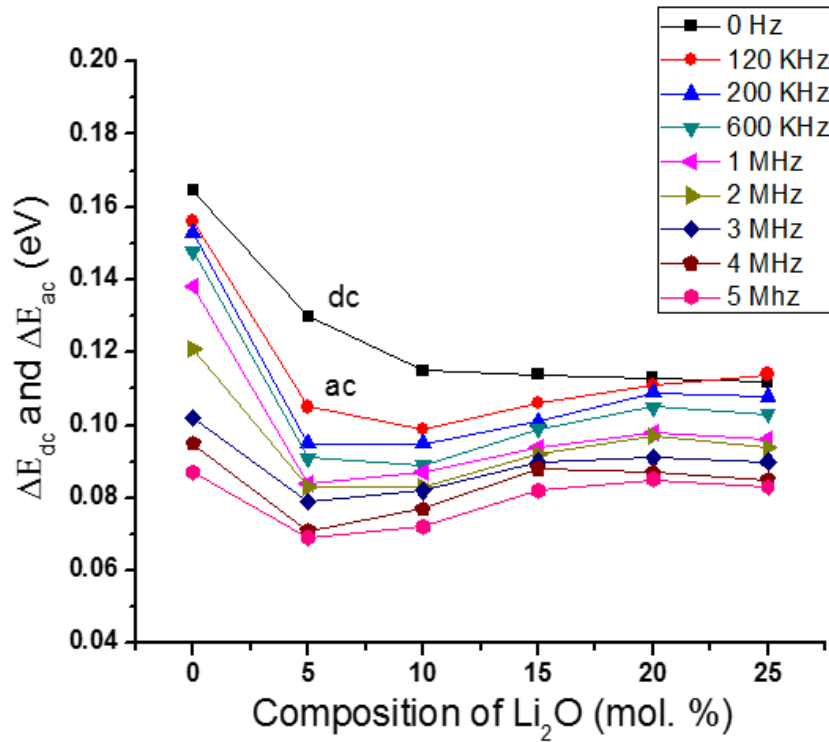
Fig.9: The variation of ac activation energies ΔE_{dc} and ΔE_{ac} with the concentration of Li_2O mol% at different frequencies.

3-4-2-3 Temperature and frequency dependence of dielectric constant ε' and ε''

The complex dielectric constant of the investigated samples is formulated with two parts, ε = ε' + i ε''; where ε' is the real part of dielectric constant and it is a measure of the energy, stored from the applied electric field in the material and identified the strength of alignment of dipoles in the dielectric. ε'' is the imaginary part of dielectric constant and it is the energy dissipated in the dielectric. ε' and ε'' were evaluated using the following relations:

$$\varepsilon' = C \, L \, / \, \varepsilon_o \, A \qquad\qquad (9)$$

$$\varepsilon'' = \varepsilon' \tan \delta \qquad\qquad (10)$$

Where C is the capacitance of the sample, ε_o is the free space permittivity, L is the sample thickness and A is the area and tan δ is the dissipation factor.

The real and imaginary parts of dielectric constant ε' and ε'' of $40P_2O_5$-$20ZnO$-$(40-x)Na_2O$-xLi_2O glass samples with different concentration of Li_2O are measured over frequency range from 50 Hz to 5 MHz.
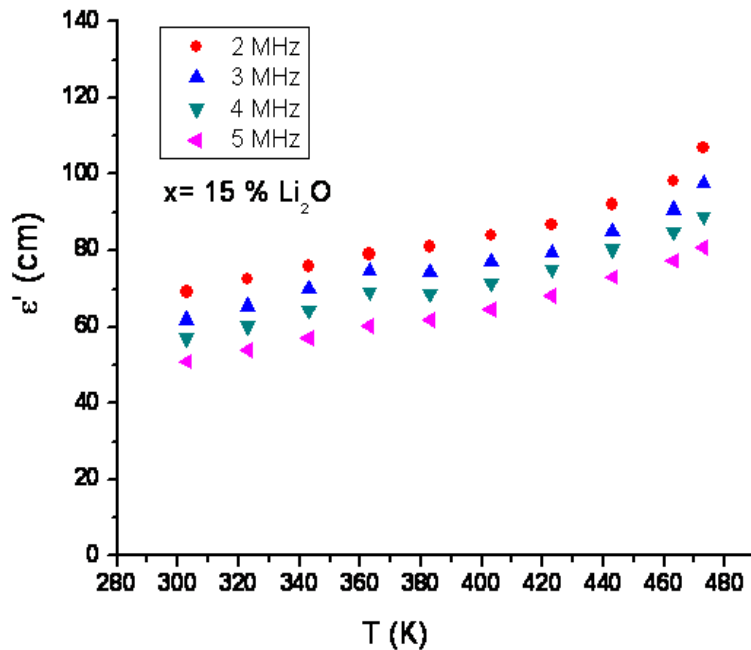
Fig.10: The temperature dependence of real part (ε') of glass containing 15 mol% Li_2O at different frequencies.

Figures 10, 11 show the variation of the real ε' and imaginary ε'' parts of dielectric constant with temperature at different frequencies for $40P_2O_5$-$20ZnO$-$(40-x)Na_2O$-xLi_2O glass. It is clear from fig.10 that he obtained plots are straight and the values of ε' increase with increasing temperature and also with decreasing frequency which is normal in oxide glasses and this cannot be taken as indication for spontaneous polarization   **[A. A. Bahgat et al. (2001)]**.
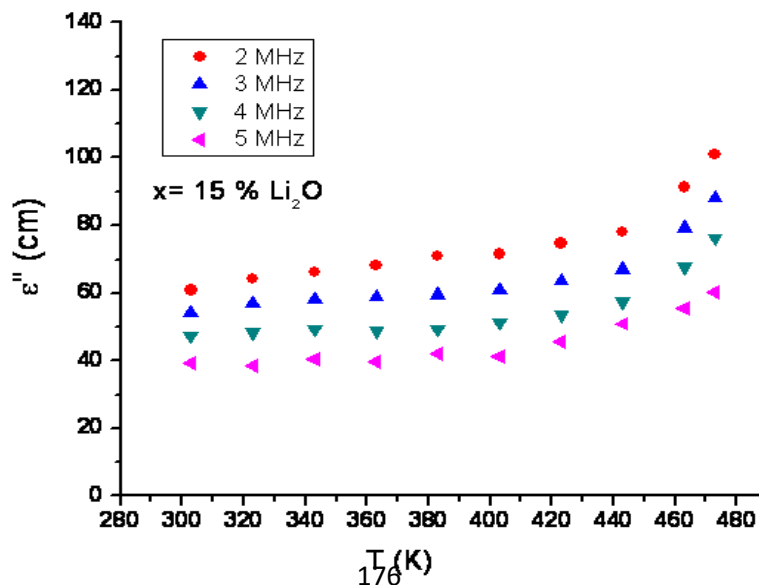
Fig.11: The temperature dependence of imaginary part (ε'') of glass containing 15 mol% Li_2O at different frequencies.

This can be explained by means of dielectric polarization mechanism of the material. Among various polarization, deformational polarization (electronic and ionic) and relaxation polarization (dipolar and space charge polarization) that contribute to the dielectric constant. Electronic and ionic polarizations are active in high frequency range, while the other two mechanisms prevail in the low frequency range **[S. Kurien et al. (2006), I. Bunget et al. (1984)]**. The increase of both ε' and ε'' toward the low frequency region may be attributed to space charge polarization. As the frequency increases, the polarizability contribution from ionic source decreases and finally disappear **[K. H. Mahmoud et al. (2011)]**.
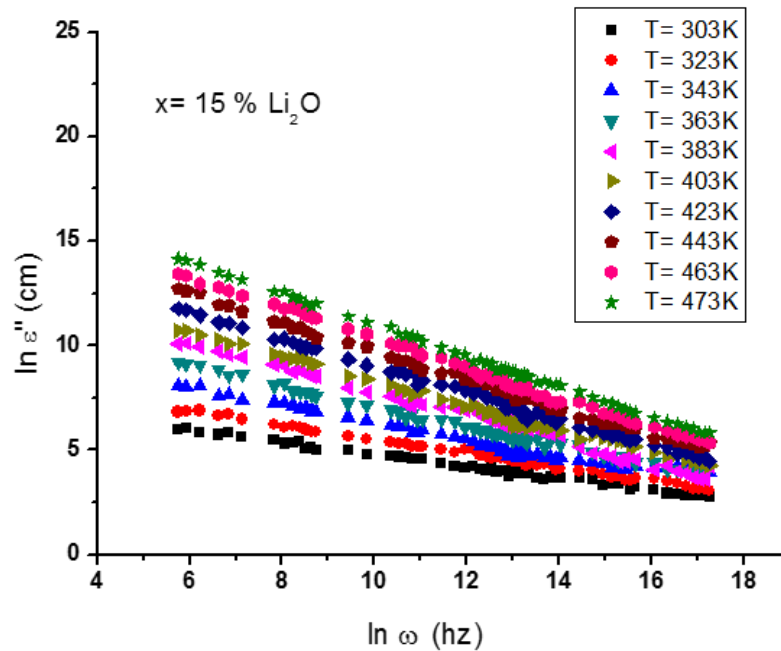

Fig.12: Frequency dependance of imaginary part (ε') of glass containing 15 mol% Li_2O at different temperatures.

Table.4: The variation of the real ε' and imaginary ε'' parts of dielectric constant at room temperature and

frequency 3 MHz on concentration of Li_2O mol%.

Composition of $40P_2O_5$-$20ZnO$-$(40-x)Na_2O$-xLi_2O x (mol %)	Real part (ε') of dielectric constants (cm)	Imaginary part (ε'') of dielectric constants (cm)
0	86.468	97.557
5	80.411	80.249
10	68.268	53.755
15	65.555	56.866
20	49.748	36.875
25	37.016	32.438

Table.4 Shows the dependence of the real ε' and imaginary ε'' parts of dielectric constant at room temperature and frequency 3 MHz on concentration of Li_2O mol%.

Fig.12 shows the variation of Ln ε'' with Ln ω for the investigated samples. It is clear from this figure that the obtained curves are straight lines at various temperatures. According to Guntini et al **[J. C. Guntini et al. (1981)]** ε'', at a particular frequency in the temperature range where dielectric dispersion occurs, is given by:

$$\varepsilon'' = B\, \omega^m \qquad\qquad (11)$$

The power m of this equation was calculated from the negative slopes of the obtained straight lines of fig.12 at different temperatures. The variation of the obtained values of m with temperature for different concentration of Li_2O is shown in fig.13. The results show that m decreases with increasing temperature and to be nearly constant with increasing concentration (table 5). According to Guintini et al the exponent m can be related to the temperature and the maximum barrier height W_m through the following equation:

$$m = -4K_B T/W_m \qquad\qquad (12)$$

It is found that the maximum barrier height W_m is nearly constant with increasing concentration.
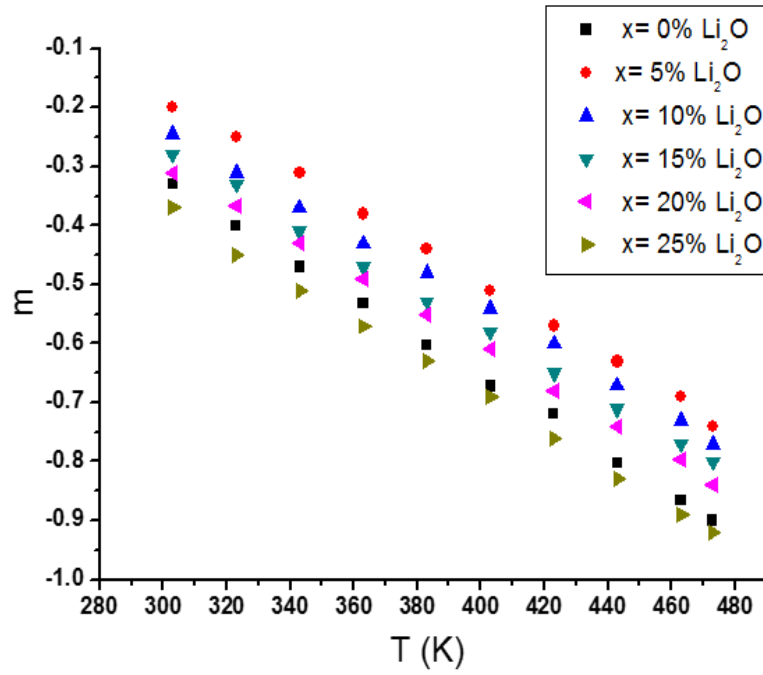
Fig.13: Temperature dependance of the investigated glasses for exponent m at different concentrations of Li_2O mol%.

Table.5: Shows the variation of the obtained values of the maximum barrier height Wm at different concentrations of Li_2O mol%.

Composition of $40P_2O_5$-$20ZnO$-$(40-x)Na_2O$-xLi_2O x (mol %)	Maximum barrier height (Wm) (eV)
0	0.099
5	0.11
10	0.110
15	0.112
20	0.111
25	0.108

4. Conclusion

Glasses of $40P_2O_5$-$20ZnO$-$(40-x)Na_2O$-xLi_2O were prepared and analyzed. All the prepared glasses are amorphous in nature. The density and oxygen packing density of the glasses increased with increasing of Li_2O content which indicates that the glass structure is more packed together. The differential thermal analysis data showed that the glass sample contains 15 mol. % Li_2O has the highest thermal stability. The conductivity in these glasses is seen to be dominated by Li_2O concentration and it is found to increase with increasing of the modifier Li_2O concentration. The dc conductivity of these glasses obeys the Arrhenius law and the values of activation energies at low and high temperatures are calculated. The values of σ_{dc} calculated also from the impedance study. Conductivity mechanism for grain resistance at room temperature was discussed using Cole-Cole plot. The ac conductivity data of investigated glasses has been fitted to a single power law equation. The exponent s is found to decrease with increase of temperature and has values between 0.89 – 0.996. Consequently the correlated barrier hopping (CBH) seems to be the most interesting model related to the obtained results. The real and imaginary parts of dielectric constant ε' and ε'' have been found to increase with increasing temperature which is normal in oxide glasses and decrease with increasing frequency which may be attributed to space charge polarization.

5. References

A. A. Bahgat, Y.M. Abou eZeid, Phys. Chem. Glasses 42 (2001) 51.

A. Bhide, K. Hariharan, Mater. Chem. Phys.105 (2007) 213.

A. Ben Rasem, F. Hlel, K. Guidara, M. Gargouri, J. Alloys Compds. 385 (2009) 718.

A. V. Chandrasekhar, A. Radhapathy, B. I. Reddy, Opt. Mater. 22 (2003) 215.

A. Yamano, M. Morishita, G. Park, T. Sakamoro, H. Yamauchi, T. Nagakane, M.Ohji,

A. Sakamoto, T. Sakai, J. Electrochem. Soc. 161 (2014) A1094-A1099.

D. Carta, J. Knowles, P. Guerry, M. Smith, R. New. Port, J. Mater. Chem., 19 (2009) 150-158.

D. E. Day, Z. Wu, C. S. Ray and P. Hrna, J. Non-Cryst. Solids, 1 (1998) 241.

D. D. Ramteke, R. E. Kroon, H. C. Swart, J. Non-Cryst. Solids 457 (2017) 157-163.

D. P. Almond, C. C. Hunter, A. R. West, J. Mater. Sci. 19 (1984) 3236.

G.E. Pike, Phys. Rev. B6 (1972) 157.

H. A. Zayed, N. F. Osman, M. M. El Okr, L. I. Soliman, accepted for publication (2356-8372), J. Sci. Res. Sci. 36 (2019).

I. Abrahams, E. Hadzifejzovic, Solid State Ionic 134 (2000) 249.

I. Bunget, M. Popescu, Phys. Solid Dielectric, Elsevier, New York, 1984.

J. C. Guntini, J. V. Zan Chetta, D. Julien, R. Eholie, P. Houenou, J. Non-Cryst. Solids 45 (1981).

K. H. Mahmoud, F. M. Abdel-Rahim, K. Atef, Y. B. Saddeek, Current Applied Physics 11(2011)55- 60.

M. J. Miah, A. K. M. Akther Hossain, Acta Metall. Sin. (Engl. Lett.) (2016).

Nehal Aboulfotoh, Yahia El bashar, Mohamed Ibrahem, Mohamed El Okr, Ceramics International 40 (2014) 10305-10399.

P. M. V. Teja, C. Rajyasree, P. S. Rao, A. R. Babu, C. Tirupataiah, D. K. Rao, J. Mol. Struct. 1014 (2012) 119-125.

Paramjyot Komar Jha, O. P. Pandey, K. Singh, J. Mol. Struct. 1094 (2015) 174-182.

R.H. Chen, R.Y. Chang, C.S. Shem, Solid State Ion. 177 (2006) 2857.

R. K. Brow, D. R. Tallant, S. T. Myers and C. C. Phifer, J. Non- Cryst. Solids, 191 (1995) 45.

R. K. Brow, J. Non-Cryst. Solids, 1 (2000) 263-264.

S. Kurien, J. Mathew, S. Sebastian, S.N. Pottv, Kc. George. Mater.Chem.Phys. 98 (2006) 470.

S. R. Elliot, Philos. Mag. B.36 (1978) 129.

S. T. Reis, M. Karabulut and D. E. Day, J. Non-Cryst. Solids, 292, 150 (2001).

Samir Y. Marzouk, Materials Chemistry and Physics 114 (2009) 188-193.

Sh. A. Mansour, I. S. Yahia, G. B. Sakr, Solid State Communication 150 (2010) 1386-1391.

Yahia H. Elbashar, Ali M. Badr, Haron A. Elshaikh, Ahmed G. Mostafa, Ali M. Ibrahim, Processing and Application of Ceramics 10 (4) (2016) 277-286.

الملخص باللغة العربية

تحضير و دراسة الخواص الكهربية لزجاجيات أكسيد فوسفات الزنك و الصوديوم المعدلة بأكسيد الليثوم

[a] نجلاء فتحى عثمان، [b] محمد محمود العقر، [c] ليلى ابراهيم سليمان، [d] حمدية عبد الحميد زايد

[a] مدرس مساعد ـ قسم الفيزياء ـ الأكاديمية الحديثة للهندسة و التكنولوجيا ـ القاهرة – مصر.
[b] استاذ فيزياء الجوامد ـ قسم الفيزياء ـ كلية العلوم ـ جامعة الأزهر ـ القاهرة – مصر.
[c] استاذ فيزياء الجوامد ـ قسم الفيزياء ـ المركز القومى للبحوث ـ القاهرة – مصر.
[d] استاذ فيزياء الجوامد ـ قسم الفيزياء ـ كلية البنات ـ جامعة عين شمس ـ القاهرة – مصر.

فى هذا البحث تم تحضير زجاج شفاف من $x Li_2O$ - $(40-x)Na_2O$ - $20 ZnO$ - $40 P_2O_5$ حيث ان (% $0 mol. \% \leq X \leq 25 mol. \%$) باستخدام تقنية الصهر و التبريد المفاجىء، و قد تاكد أن الزجاج المحضر ذات طبيعة امورفيه من خلال استخدام تقنيه حيود اشعة اكس (XRD)، و قد وجد أنه بزياده تركيز Li_2O تزيد كل من الكثافة (ρ) و كثافة الحزمة الأوكسجينية (OPD) بينما الحجم المولارى (V_m) يقل و هذا يؤكد ان الزجاج اصبح اكثر ترابطا. اظهرت دراسات التحليل الحرارى التفاضلى (DTA) أن اعلى درجه ثبات حرارى عند تركيز % $15 mol.$ و ان درجة التحول للزجاج (T_g) تقل مع زيادة تركيز Li_2O. تم دراسة الخواص الكهربية لكل من التيار المستمر و التيار المتردد وتم تعيين معاملات ثابت العزل ε' و ε''، و من الدراسة تم تعيين طاقتي التنشيط ΔE_{dc1} عند درجات الحرارة المرتفعة (473 - 403 K) و ΔE_{dc2} عند درجات الحرارة المنخفضة (303 - 383 K) و ايضا قد تم تعيين σ_{dc} عند درجات حرارة مختلفة و تركيزات مختلفة بأستخدام Cole-Cole plot و كذلك تم تعيين ΔE_{ac}. لتعيين ميكانيكية التوصيل تم دراسة تغير الموصلية الكهربية للتيار المتردد مع درجة الحرارة عند ترددات مختلفة و تم تحليلها علي اساس correlated barrier hopping (CBH)، وقد وجد ان قيم exponent (s) تتراوح ما بين – 0.996 0.89، و بناءً عليه يعتبر (CBH) هو انسب موديل متفق مع النتائج، و قد وجد من دراسة معاملات ثابت العزل ε' و ε'' انها تقل مع زيادة الترددات المختلفة و الحرارة و تم شرح هذه النتائج بواسطة dielectric polarization mechanism of material. كذلك تم حساب قيمة maximum barrier height (W_m) بأستخدام معادلات Guitini و وجد انه يزداد بزيادة $Li_2O mol\%$.